

Perpendicular magnetic anisotropy and temperature-dependent reorientation transition of the magnetization in CeH₂/Fe multilayers

O. Schulte, F. Klöse,* and W. Felsch

I. Physikalisches Institut, Universität Göttingen, Bunsenstr. 9, 37073 Göttingen, Germany

(Received 20 March 1995)

Magnetic anisotropies were investigated in a series of CeH₂/Fe multilayers with a pronounced (111) texture by measurements of the magnetization between 4.2 and 300 K. The results reveal, together with ⁵⁷Fe Mössbauer spectra measured previously, that in the ground state at low temperatures the magnetization is oriented perpendicular to the layer planes in a multidomain configuration, up to remarkably large Fe layer thicknesses. It is demonstrated in a phenomenological model that this appears as the result of a strong interface anisotropy in combination with a magnetostatic interaction between the domains in the Fe layers across the CeH₂ layers, which overcome the shape anisotropy of the Fe layers. At a critical temperature T_R , which decreases with both the Fe or CeH₂ layer thicknesses t_{Fe} and t_{CeH} , a transition from the out-of-plane to an in-plane orientation of the magnetization is observed. The present system is outstanding among other rare-earth/iron multilayers, because the reorientation transition occurs rather abruptly in a narrow temperature range.

I. INTRODUCTION

Among the novel properties of thin ferromagnetic films and multilayer structures the phenomenon of perpendicular magnetic anisotropy has attracted much attention in recent years.¹ It has been attributed to a strong surface or interface anisotropy which may counteract the shape anisotropy and may lead to an easy axis for the magnetization normal to the film planes. While shape anisotropy arises from the long-range magnetic dipole interaction which favors an in-plane orientation of the magnetization, the underlying mechanisms for the surface or interface anisotropies remain, in essence, to be elucidated. Such anisotropies were recognized by Néel² as a consequence of symmetry breaking at the film boundaries. In the meantime, the physical basis for this argument has been thoroughly considered in numerous theoretical publications,³ and it has been recognized in the case of multilayers that, in addition to the effects from the reduced coordination of the atoms at the interfaces, the altered electronic structure⁴ and magnetostrictive elements activated by epitaxial strain at the lattice-mismatched boundaries^{5,6} may contribute considerably to the interface anisotropy.

As the perpendicular magnetization state of the layers originates from the competing interplay of a volume and a surface or interface contribution, it is clear that with increasing film thickness a reorientation of the magnetization must occur, from normal to in-plane alignment. Remarkably, this reorientation transition can be driven not only by an increase of film thickness but also of temperature.⁷⁻⁹ This has stimulated considerable activity¹⁰ to calculate the anisotropic part of the free energy, which is responsible for the existence of easy magnetization directions. It has been argued,^{11,12} that the directional entropy may significantly contribute to the free energy at higher temperatures and hence may be important for the

thermally activated reorientation of the magnetization.

The perpendicularly magnetized state is of particular relevance for the technology of high-density magnetic recording. This raises the question about the microscopic domain structure in the magnetic layers. Here, experimental methods developed in recent years have provided new insights. In contrast to the early study of Kittel¹³ predicting a single-domain state to be the energetically preferred ground state in the case of a thin film with a perpendicular magnetic easy axis, recent experiments on ultrathin epitaxial films¹⁴ and on multilayers¹⁵ have shown multidomain configurations to be a quite common feature. This corroborates calculations for thin films¹⁶⁻¹⁸ and multilayers¹⁹ performed more recently.

A special class among the magnetic layer systems are those combining transition metals and rare-earth elements. Frequently quoted examples showing perpendicular magnetic anisotropy are Tb/Fe (Refs. 20 and 21) and Nd/Fe (Refs. 22 and 23) multilayers. For these systems, effects from the crystalline electric field at the interfaces acting on the aspherical *4f* charge distribution of the rare-earth atoms have been invoked to explain the perpendicular orientation of the magnetization.^{22,24} In this paper we report on the observation of perpendicular magnetic anisotropy in a multilayer structure of cerium hydride and iron, CeH₂/Fe. Here, the presence of hydrogen is essential for this phenomenon, since in bare Ce/Fe multilayers the magnetic anisotropy is dominated by the shape anisotropy and hence the magnetization is confined to the layer planes.²⁵ The introduction of hydrogen into this layer system does not only change the magnetic properties,^{26,27} but leads also to a profound modification of the structural^{26,28} and mechanical properties.²⁹ The main experimental results found for the CeH₂/Fe multilayers which will be discussed are as follows.

(i) The Fe layers, if suitably textured, are subjected to a strong interface anisotropy.

(ii) At a critical temperature, the magnetization changes from out-of-plane to in-plane orientation. This reorientation temperature depends on the thickness of both the Fe and the CeH₂ layers.

(iii) The perpendicularly magnetized ground state is characterized by a multidomain configuration.

(iv) The magnetostatic interaction between the perpendicular domains in the Fe layers across the CeH₂ layers adds to the stabilization of this configuration.

II. EXPERIMENTAL DETAILS AND SAMPLE CHARACTERISTICS

The multilayers were prepared by reactive ion-beam sputtering using argon in an ultrahigh vacuum chamber, at a hydrogen partial pressure of 8×10^{-6} mbar. The base pressure was below 5×10^{-10} mbar prior to the introduction of hydrogen, partial pressures of residual gases (O₂, N₂, H₂O, for example) were below 10^{-10} mbar during deposition. Only the cerium layers absorb hydrogen, favored by a large negative enthalpy of mixing. Subsequent analysis by the (p, γ) resonant nuclear reaction of ¹⁵N with hydrogen revealed that the stoichiometry of the hydride is close to CeH₂,³⁰ in good agreement with former estimates based on specific-heat and resistivity measurements.²⁶ Si(100) wafers coated with a 40 Å thick Cr buffer layer were used as substrates. (Some of the previous measurements quoted here were carried out on samples deposited on Cr-coated Kapton foil or quartz glass. But comparative studies testify that, because of the same buffer layer, the properties of the multilayers do not depend on the special kind of substrate.) Growth rates varied from 0.3 Å/s for CeH₂ to 0.7 Å/s for Fe. Two series of heterostructures were investigated, with either a constant Fe or CeH₂ layer thickness of 16 Å. The total multilayer thickness was near 2000 Å. The samples were covered with a 100 Å thick Cr layer to protect them from oxidation on exposure to atmosphere.

The structure of the multilayers was characterized by x-ray diffraction in Bragg-Brentano θ - 2θ geometry and by reflection high-energy electron-diffraction (RHEED) diagrams taken *in situ*. The samples for the present study were deposited at room temperature, in contrast to the previously investigated ones²⁶ which were grown at 90 K. Up to a critical thickness, which is near 10 Å for room-temperature deposition, the individual CeH₂ and Fe layers grow in an amorphous structure. Above this thickness, the Fe layers (bcc structure) show the usual (110) texture if grown at low-temperature and a pronounced (111) texture if grown at room temperature. The CeH₂ sublayers (fcc structure) are always (111) textured. According to the RHEED diagrams, there is a high degree of lateral order in the CeH₂ and Fe layers deposited at room temperature [(111) orientation]. Presumably, this originates from the relatively small mismatch between the (111) planes: the Ce-Ce distance in CeH₂ is about 3% smaller than the Fe-Fe distance. However, because of a missing epitaxial relation between the first deposited

CeH₂ layer and the Cr-coated Si substrate, coherent growth across the CeH₂-Fe interfaces could not be achieved; no satellites are visible near the (111) reflections in the x-ray diagrams. The structural coherence length in the multilayers parallel to their growth direction, as determined from the linewidths of the Bragg peaks, corresponds to the thickness of the individual layers. Rocking curves on the CeH₂ (111) and the Fe (222) peaks show full width at half maximum of typically 7° and 4°, respectively.

The film thickness limiting amorphous growth of CeH₂ and Fe with (111) texture (~ 10 Å) is unusually low as compared to other layered structures combining rare-earth and transition metals. In the case of Fe, for example, this thickness ranges between 20 and 30 Å in association with many different rare earths.^{25,31,32} It has been suggested³¹ that in such heterostructures growth in the amorphous phase originates in the large mismatch between the interatomic distances at the interface between the rare-earth and the transition metal, but a fundamental understanding of how this affects the growth mode is lacking. The distinctly reduced limiting thickness value for the CeH₂/Fe system, where the mismatch is relatively small in the case of (111)-textured Fe layers, lends support to the proposed hypothesis. Here, only the crystalline layers will be considered. It is an advantage that the combination of CeH₂ and Fe offers the opportunity to study crystalline bcc Fe (especially its magnetic properties) in the (111) texture, which is not commonly encountered, down to small layer thicknesses in conjunction with a rare earth.

Special efforts were made to clarify the microscopic structure of the CeH₂/Fe interfaces. The measured small-angle x-ray-diffraction diagrams were modeled by means of Monte Carlo simulations, as described in detail by Klose *et al.*²⁸ It results (for sublayer thicknesses above 10 Å) that diffusion is negligible and that roughness, if quantified by a Gaussian fluctuation of the local layer thickness, is restricted to 1.0 atomic layer. This reveals that we deal with a well-defined layer structure with a sharp composition profile. This is corroborated by ⁵⁷Fe Mössbauer spectroscopy.²⁷ Compared to the Ce/Fe multilayers, the introduction of hydrogen into the Ce sublayers leads to a sensible sharpening of the interfaces and to a remarkable modification of the electronic structure of the interfacial Ce atoms: while in the former system the ground state of these atoms is α -Ce-like with itinerant 4*f* states³³ it is γ -Ce-like in the CeH₂/Fe multilayers, i.e., we have localized 4*f* states throughout the entire extension of the CeH₂ sublayers.³⁴

The magnetization of the samples was measured by means of a vibrating-sample magnetometer between liquid-helium and room temperature, in magnetic fields up to 50 kOe applied parallel and perpendicular to the layer planes. The measurements along these two orthogonal field directions permit to determine the uniaxial magnetic anisotropy. Further information was deduced from the magnetic susceptibility measured in an effective ac magnetic field of 3 Oe, at a frequency of 117 Hz, oriented in the film planes.

III. RESULTS AND DISCUSSION

All CeH_2/Fe multilayers with crystalline iron [$t_{\text{Fe}} \geq 10 \text{ \AA}$, bcc-(111) texture] show ferromagnetic behavior and can be magnetically saturated in the fields available. The measured saturation magnetization at 4.2 K referred to the Fe part, $M_{S,\text{Fe}}$, agrees with the value of bulk $\alpha\text{-Fe}$ (1742 emu/cm^3 at 4.2 K) within the error bars. Within the temperature range from 4.2 up to 300 K, it decreases by a few percent and obeys a Bloch spin-wave law

$$M_{S,\text{Fe}}(T) = M_{S,\text{Fe}}(0)(1 - bT^{3/2}) \quad (1)$$

with, for instance, $b = 1.9 \times 10^{-5} \text{ K}^{-3/2}$ for the multilayer $[16 \text{ \AA CeH}_2/16 \text{ \AA Fe}] \times 150$, corresponding to a 10% decrease of M_S between 4.2 and 300 K. The spin-wave parameter b increases with decreasing thickness of the Fe layers t_{Fe} and exceeds the value of bulk iron ($5.2 \times 10^{-6} \text{ K}^{-3/2}$). This points to a reduced Curie temperature compared to $\alpha\text{-Fe}$, a behavior which must be interpreted as a size and/or interface effect.

CeH_2/Fe multilayers with amorphous iron ($t_{\text{Fe}} < 10 \text{ \AA}$) exhibit magnetic ordering temperatures below room temperature (near 200 K), a distinctly reduced Fe saturation magnetization and a considerable high-field magnetic susceptibility. This addresses the problem of the magnetic properties of the amorphous Fe phase which will not be discussed here. In the following we restrict ourselves to the multilayers with crystalline Fe sublayers showing (111) texture, especially to their magnetic anisotropy.

Important information about the orientation of the spontaneous magnetization in the ground state of the CeH_2/Fe multilayers and thereby about the effective anisotropies results from ^{57}Fe Mössbauer spectroscopy. This has been discussed recently at some length.²⁷ The intensity ratio of the six lines in the magnetically split spectra is given by $3:X:1:1:X:3$, where the relative intensity X of the $\Delta m = 0$ transitions (second and fifth line) is connected with the angle θ between the directions of the incident γ rays (here in the film normal) and the Fe-atom magnetic moments according to

$$X = \frac{4 \sin^2 \theta}{1 + \cos^2 \theta} \quad (2)$$

In Fig. 1, the values of X and θ resulting from the Mössbauer transmission spectra²⁷ of a multilayer $[16 \text{ \AA CeH}_2/16 \text{ \AA Fe}] \times 150$ are plotted as a function of temperature. For low temperatures, we have $X = 0$ ($\theta = 0^\circ$) which reveals that the spontaneous Fe magnetic moments are oriented perpendicular to the film plane. The fact that the Fe layer magnetization is directed fully out of plane is a signature of a strong perpendicular anisotropy. For high temperatures, we have $X = 4$ ($\theta = 90^\circ$) and hence the Fe moments lie in the film plane. The reorientation transition occurs near 170 K within a remarkably narrow temperature interval (see also Fig. 7, below). The Mössbauer spectra, taken in zero external magnetic field, do not allow to distinguish between a uniformly magnetized remanent state and a configuration of antiparallel domains. This simply results from Eq. (2) which only contains the squared goniometric functions.

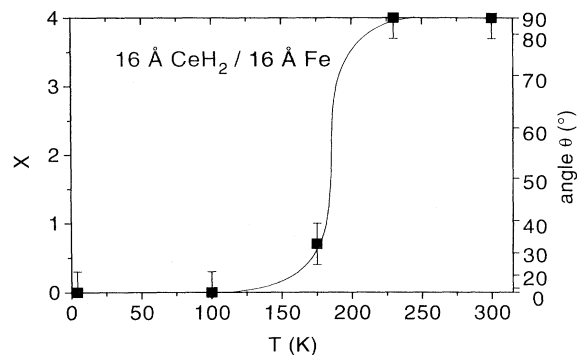


FIG. 1. Relative intensity X of the second and fifth line of ^{57}Fe Mössbauer transmission spectra (deduced from Ref. 27) of a multilayer $[16 \text{ \AA CeH}_2/16 \text{ \AA Fe}] \times 150$ and angle θ between the directions of the Fe moment and the film normal [Eq. (2)] as a function of temperature T . The line is a guide to the eye.

Information about a possible domain structure in the multilayers can be deduced from measurements of the magnetization. As a representative example for the samples investigated, we show in Fig. 2 the magnetization curves of a multilayer with the same composition as in Fig. 1, measured at different temperatures along both the in-plane and perpendicular directions. It is evident that these curves are very different for the two field orientations. They reveal (i) the crossover from a state with perpendicular magnetic anisotropy prevailing at low temperatures to a state with in-plane anisotropy at high temperatures, as it is evidenced by the change in the peak ratios of the Mössbauer spectra, and (ii) the presence of a magnetic multidomain structure in the ground state of the layers, at least for the case with perpendicular magnetization. The first property can be conjectured from the relative magnitude and the variation with temperature of the

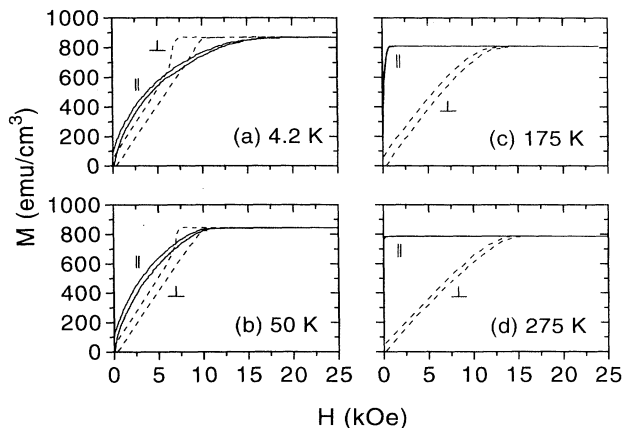


FIG. 2. Magnetization curves of a multilayer $[16 \text{ \AA CeH}_2/16 \text{ \AA Fe}] \times 62$ in a magnetic field H applied parallel (full line) and perpendicular (dashed curve) to the film plane at different temperatures [(a)–(d)]. The magnetization M is referred to the total volume.

magnetic saturation fields, the second one from the low remanence and small hysteresis. The latter features indicate a state of nearly complete demagnetization of the multilayers in zero external field. In the in-plane case, this may also be a consequence of an antiparallel orientation of adjacent Fe layers. Such coupling has been observed recently by small-angle neutron reflectometry for a suitable thickness of the CeH_2 spacer layers and magnetic fields below 200 Oe.³⁵

It is characteristic that at 4.2 and 50 K, where according to the Mössbauer spectra the Fe magnetic moments unambiguously point perpendicular to the film planes, the magnetization increases linearly with the field applied in the perpendicular direction and saturates only near 10 kOe [Figs. 2(a) and 2(b)]. We shall argue in the following that this shearing of the magnetization curves from a steplike increase ideally expected along the easy direction is a signature of a magnetostatic effect arising from domains. It can be concluded then that, at low temperatures and in zero magnetic field, we have a configuration of domains magnetized alternately up- and downwards along the film normal.

The shape of the in-plane magnetization curves is quite different from the perpendicular ones. They exhibit large saturation fields at low temperatures and are strongly affected by raising the temperature. At the reorientation transition near 170 K, the parallel curves become almost rectangular and remain more or less unchanged up to room temperature, reflecting that now the magnetization spontaneously lies in the film plane [Figs. 2(c) and 2(d)].

The configuration of magnetic domains in ultrathin films and multilayers, which results from the balance between the magnetostatic and domain-wall energies, is a matter of considerable interest, especially in the case of layers with a perpendicular easy axis. For this anisotropy, Yafet and Gyorgy¹⁶ predicted, in a zero-temperature variational approach, that a pattern of stripe domains being magnetized alternately up and down should represent the ground state of films a few monolayers thick, above a certain threshold value for the ratio of perpendicular-anisotropy to demagnetization energy. A similar result was found by Kashuba and Pokrovsky¹⁷ in a finite-temperature renormalization-group analysis. Recently, Alenspach *et al.*¹⁴ have observed, using spin-polarized scanning electron microscopy, that ultrathin ferromagnetic films with an out-of-plane easy axis generally show up and down domains of irregular shape, with drastic variations in size from system to system (typically, the variations are between a few μm and some $10 \mu\text{m}$). In contrast, films with in-plane anisotropy are single domain over areas approaching the lateral dimensions of the sample. The stripe-domain state could be observed only near the reorientation temperature where surface and shape anisotropies almost compensate. Barnes *et al.*¹⁵ have used magnetic force microscopy to show that in Co/Pd multilayers with perpendicular anisotropy and qualitatively similar perpendicular magnetization curves as in Figs. 2(a) and 2(b) the domains appear as stripe domains. The repetition length of adjacent up and down stripe domains varies between 180 and 450 nm.

Suna³⁶ has adapted the domain model of Kooy and

Enz³⁷ for a perpendicular magnetic ground state of a single thin plate to evaluate the magnetostatic energy in a multilayer consisting of alternating ferromagnetic and nonmagnetic layers. He assumed that (i) the magnetization, directed perpendicular to the planes, is arranged in alternately polarized domains in the form of stripes, and (ii) the domain walls are freely mobile. Within the limit that the domains are large compared to the thickness of the magnetic layers but small compared to the total thickness of the layered stack, it simply results that the multilayer behaves like a uniform medium and the magnetostatic interaction between the domains can be derived in a continuum approach. The energy per unit volume required to saturate the sample perpendicularly to the film plane, starting from a multidomain state, then amounts to $2\pi M_S^2$, where M_S denotes the saturation magnetization referred to the total multilayer volume. Hence, magnetic saturation is reached in a perpendicular magnetic field $H_S^\perp = 4\pi M_S$. From this result Suna inferred the following rule of thumb to interpret the perpendicular

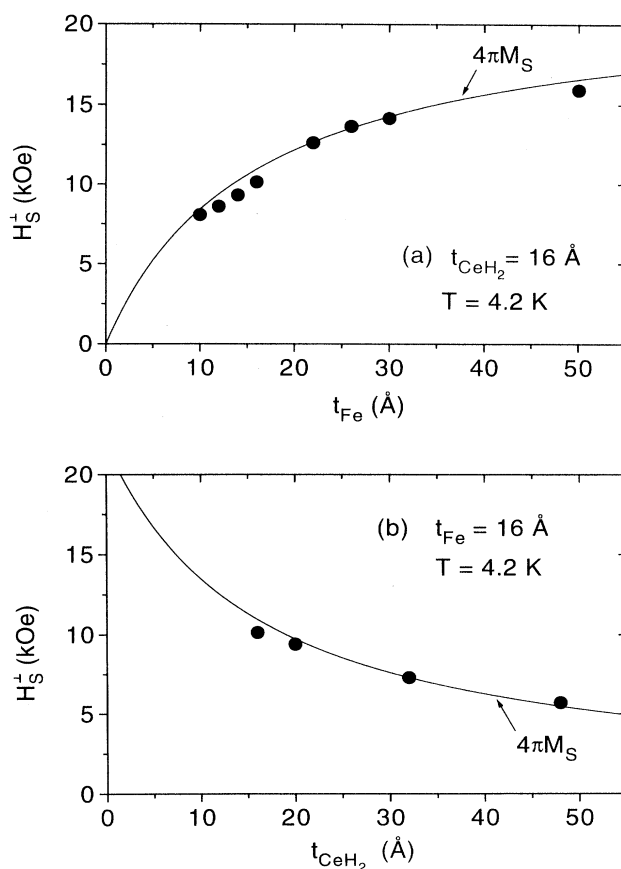


FIG. 3. Magnetic saturation field H_S^\perp deduced from the perpendicular magnetization curves at 4.2 K and $4\pi M_S = 4\pi M_{S,Fe} t_{Fe} / \Lambda$ (solid lines) of CeH_2/Fe multilayers (with saturation magnetizations M_S referred to the total volume and $M_{S,Fe} = 1742 \text{ emu/cm}^3$ of bulk iron at 4.2 K) as a function of (a) the Fe-layer thickness t_{Fe} at 16 Å thick CeH_2 layers and (b) the CeH_2 layer thickness t_{CeH_2} at 16 Å thick Fe layers. The total multilayer thickness is $\approx 2000 \text{ \AA}$.

magnetization curves of a multilayer with respect to its ground state: $H_S^\perp \leq 4\pi M_S$ points to perpendicularly magnetized stripe domains, whereas $H_S^\perp > 4\pi M_S$ indicates that the magnetization lies in the film plane.

The values of H_S^\perp and $4\pi M_S$, measured at 4.2 K for both series of samples, are compared in Fig. 3 as a function of the individual Fe and CeH₂ layer thicknesses t_{Fe} and t_{CeH} , respectively. (We have $M_S = M_{S,\text{Fe}} t_{\text{Fe}} / \Lambda$, where $M_{S,\text{Fe}}$ agrees with the saturation magnetization of bulk Fe and $\Lambda = t_{\text{Fe}} + t_{\text{CeH}}$ is the modulation length of the multilayers.) As can be seen, H_S^\perp is very close to $4\pi M_S$ for all thickness combinations studied. Obviously, the model proposed by Suna³⁶ describes the magnetic ground state of the CeH₂/Fe multilayers in a correct way: at 4.2 K and in zero applied magnetic field, we have a configuration of domains magnetized up and down along the film normal. The restriction of the model imposed onto the lateral size D of such domains with respect to the thickness of the individual ferromagnetic layers and the whole multilayers enables us conversely to roughly estimate the upper and lower bound of D of the CeH₂/Fe system: D should range between the maximum thickness of the Fe layers and the total thickness of the multilayers, i.e., $50 \text{ \AA} \ll D \ll 2000 \text{ \AA}$.

The shape of the perpendicular magnetization curves at low temperatures [Figs. 2(a) and 2(b)] indicates that magnetization reversal mainly occurs by nucleation and subsequent domain-wall motion. The nucleation process is characterized by a distinct knee in the magnetization curve appearing as the applied field is reduced from the saturation value. Upon further reduction of the field, the domain walls are relatively free to move through the layers. This is evident from the small hysteresis together with the linear variation of the magnetization, which indicates that the domain-wall pinning forces are small and most of the magnetization processes are reversible. We recall that this is one of the prerequisites of Suna's model. The nucleation field strength decreases with decreasing Fe layer thickness and increases with rising temperature to eventually approach H_S^\perp . The latter observation points to a thermally activated process, but the mechanisms for the nucleation of domains in magnetic thin films are difficult to elucidate. Domains often nucleate at defects, and usually little is known about their number and distribution. In addition, details of the domain structure may be important.

The in-plane magnetization curves at low temperatures [Figs. 2(a) and 2(b)] obtained by applying the magnetic field in the hard direction, reflect a magnetization process evolving from a perpendicular multidomain ground state into a field-induced in-plane single-domain state. The totally different shapes of the curves indicate that in this case rotation of the magnetization within the domains is the dominating process in the magnetic response to the applied field.

In the plots of the magnetization versus applied field, $M(H)$, (Fig. 2) the area enclosed by the magnetization curve and the magnetization axis up to saturation is a measure of the difference in energy density between the multidomain magnetic ground state and the field-induced single-domain state. In the case of perpendicularly ap-

plied fields, this quantity is essentially independent of temperature up to the reorientation at T_R and close to $2\pi M_S^2$, as is expected from Suna's model. Above T_R , it exceeds this value, i.e., $H_S^\perp > 4\pi M_S$, since now the state with the in-plane orientation of the magnetization has a lower energy. The area enclosed by the perpendicular and parallel magnetization curves represents the effective magnetic anisotropy K_{eff} . It denotes the difference in energy per unit volume between the single-domain configurations magnetized parallel and perpendicular to the layer planes. It has been shown³⁸ that phenomenologically K_{eff} can be decomposed into a volume and a surface or interface contribution K_V and K_S , respectively, in the present case according to

$$K_{\text{eff}} \Lambda = K_V t_{\text{Fe}} + 2K_S. \quad (3)$$

In this equation, K_{eff} is referred to the total volume and K_V to the Fe layer volume of the multilayers; $K_{\text{eff}} > 0$ is assigned to the case of a perpendicular magnetic ground state. The volume anisotropy term K_V is usually dominated by the shape anisotropy. A positive interface term, $K_S > 0$, favors perpendicular anisotropy.

Figure 4 shows the quantity $K_{\text{eff}} \Lambda$ as a function of t_{Fe} for multilayers with $t_{\text{CeH}} = 16 \text{ \AA}$ at several temperatures. The linear relation of Eq. (3) is well obeyed. The slope of the straight line, i.e., K_V , coincides with the shape anisotropy ($-2\pi M_{S,\text{Fe}}^2$) of the Fe layers. Other volume contributions as, for example, magnetocrystalline and magnetoelastic anisotropies are, if present, very small. The interface anisotropy K_S is always positive and varies with temperature (Fig. 4, inset). This changes the relative weight of the volume and interface anisotropies as the temperature increases, and eventually leads to the reorientation transition of the magnetization. Within this phenomenological approach, the effect of temperature is attributed to the variation of the interface anisotropy K_S .

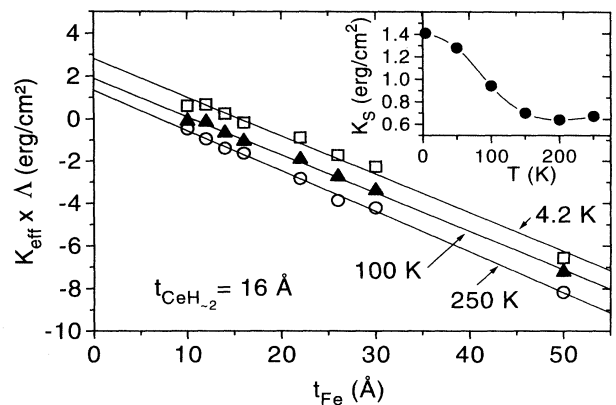


FIG. 4. Product of effective magnetic anisotropy energy density K_{eff} and modulation length Λ versus Fe layers thickness t_{Fe} [Eq. (3)] for CeH₂/Fe multilayers (total thickness $\approx 2000 \text{ \AA}$) with 16 \AA thick CeH₂ layers at three selected temperatures. The inset shows the temperature dependence of the interface anisotropy K_S , resulting from the intersection of the ordinate with the straight lines fitted to the data. The solid line in the inset is a guide to the eye.

The absolute value of K_S is in the order of 1 erg/cm² which is close to what has been observed frequently in layered Fe systems with perpendicular anisotropy.¹ But it must be noted that the mechanisms activating surface or interface anisotropies may be of very different nature in such systems. Furthermore, it is well known that K_S depends sensitively on the structural properties of the interfaces which are largely affected, for instance, by the conditions during preparation. There is evidence that in the CeH₂/Fe multilayers a magnetoelastic effect plays an important role.³⁹

Figure 4 reveals that positive values of the effective anisotropy K_{eff} are only found for Fe layers below a very small critical thickness: it amounts to about 16 Å at 4.2 K and decreases for higher temperatures. But it is clear that these values must be different from the Fe layer thicknesses limiting the observation of a perpendicularly magnetized ground state which in fact are considerably larger. To see this, we recall that K_{eff} compares the energies of the two single-domain states with perpendicular and in-plane magnetizations. However, as we have outlined above, the energetically preferred ground state below the reorientation temperature is a perpendicular multidomain state which is, by an amount of $2\pi M_S^2$, lower in energy than the magnetically saturated perpendicular state. Hence, the effective magnetic anisotropy being relevant for the observations on the present layer system is the quantity $K_{\text{eff}} + 2\pi M_S^2$. It is illustrated in Fig. 5 as a function of temperature for several layer-thickness combinations. It compares the states with perpendicular multidomain and in-plane single-domain configurations. Positive and negative values of $K_{\text{eff}} + 2\pi M_S^2$ distinguish between the out-of-plane and in-plane magnetic ground state.

As we have mentioned above, the parallel magnetization curves adopt an almost rectangular shape at the reorientation transition. This can be exploited to get access to the reorientation temperature T_R rather directly by a measurement of the magnetization in a low constant magnetic field as a function of temperature. Figure 6 shows such experimental curves for a field of 90 Oe ap-

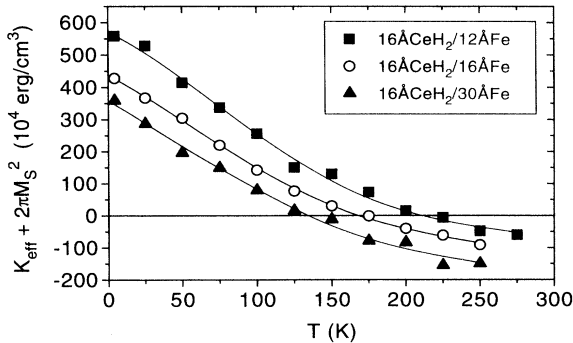


FIG. 5. Sum of the effective magnetic anisotropy K_{eff} and the magnetostatic interaction energy $2\pi M_S^2$ versus temperature for several CeH₂/Fe multilayers (total thickness ≈ 2000 Å, saturation magnetization M_S referred to the total volume). The solid lines are guides to the eye.

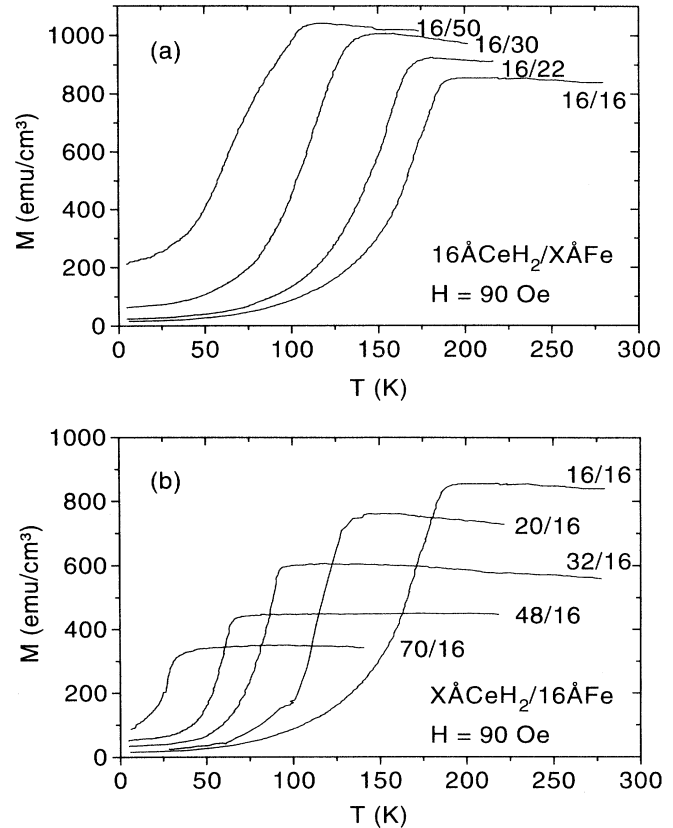


FIG. 6. Magnetization as a function of temperature in a magnetic field $H=90$ Oe applied in the film plane for several CeH₂/Fe multilayers with a constant CeH₂ layer thickness of 16 Å (a) and a constant Fe layer thickness of 16 Å (b).

plied in the layer planes. The dependence of the magnetic history is very small. After a gradual increase, the curves exhibit a rather abrupt change to a plateau. The position of this kneelike feature is identified with T_R . This temperature depends not only on thickness of the Fe layers, t_{Fe} , [Fig. 6(a)] but also on the thickness of the CeH₂ layers, t_{CeH} [Fig. 6(b)]. Similar informations result from measurements of the magnetic susceptibility in a small ac field (3 Oe, 117 Hz) applied along the layer planes. This quantity, as a function of temperature, shows a steplike increase at the reorientation transition (Fig. 7). This demonstrates, similarly as the variation of the Mössbauer spectra (Fig. 1), that the transition is remarkably sharp. It is clear that above T_R where the magnetization lies in the layer planes the magnetic response to the small ac field must depend on details of the hysteresis loops. To establish a magnetic phase diagram for the CeH₂/Fe multilayers, we display in Fig. 8 the T_R values resulting from the low-field magnetization and susceptibility data (Figs. 6 and 7) as a function of t_{Fe} at constant t_{CeH} , and as a function of t_{CeH} at constant t_{Fe} . It can be seen that the functional forms $T_R \propto t_{\text{Fe}}^{-1} + \text{const}$ and $T_R \propto t_{\text{CeH}}^{-1}$ give an excellent fit to the data, i.e., in both cases, T_R varies linearly with the reciprocal layer thickness.

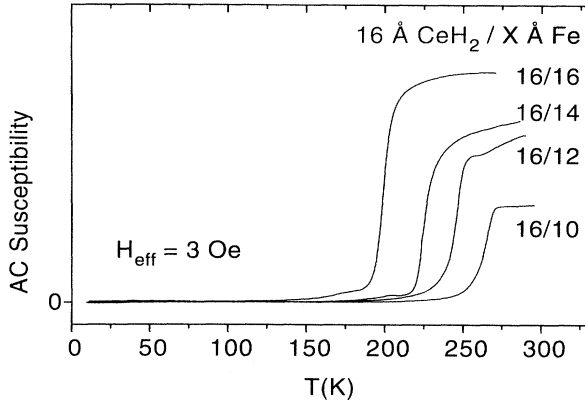


FIG. 7. Magnetic susceptibility of CeH₂/Fe multilayers (total film thickness ≈ 2000 Å) with 16 Å thick CeH₂ layers measured in an ac magnetic field ($H_{\text{eff}} \approx 3$ Oe, $\nu = 117$ Hz) applied in the film plane as a function of temperature.

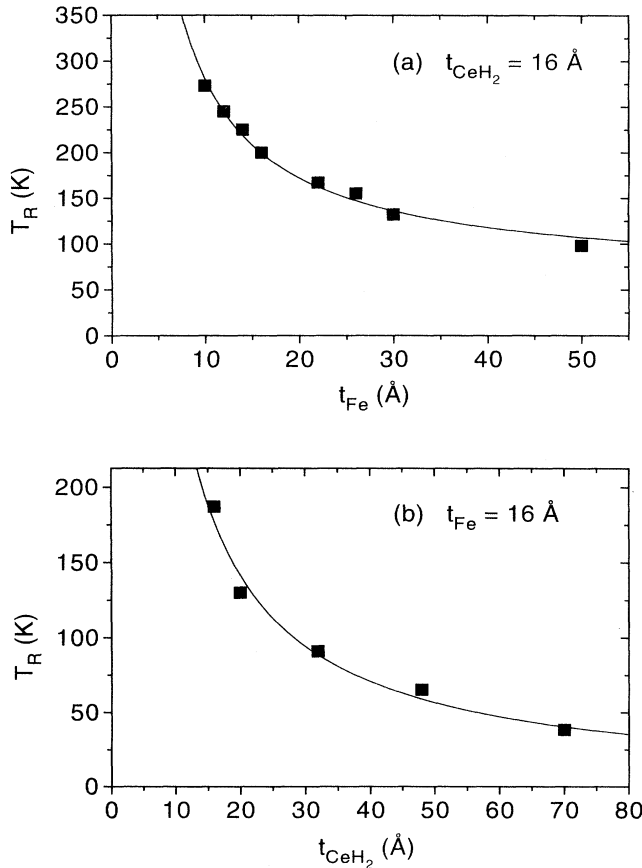


FIG. 8. Reorientation temperature T_R of the spontaneous magnetization of CeH₂/Fe multilayers versus Fe layer thickness t_{Fe} for 16 Å thick CeH₂ layers (a) and versus CeH₂ layer thickness for 16 Å thick Fe layers (b). The lines representing $T_R(t_{\text{Fe}}) = (2272 \text{ K Å})/t_{\text{Fe}} + 63.5 \text{ K}$ and $T_R(t_{\text{CeH}_2}) = (2829 \text{ K Å})/t_{\text{CeH}_2}$ are fits to the data in (a) and (b), respectively.

In the phenomenological interpretation of the magnetic anisotropy in the CeH₂/Fe multilayers we have discussed, the stability of the perpendicular magnetic multidomain ground state at low temperatures, described by the criterion $K_{\text{eff}} + 2\pi M_S^2 > 0$, is attributed to an interface contribution to the anisotropy, K_S , and an additional volume contribution, $2\pi M_S^2$, resulting from the magnetostatic interaction of the domains. At T_R , these terms are balanced by the shape anisotropy of the Fe layers, $2\pi M_{S,\text{Fe}}^2$. Hence, T_R results implicitly from the condition

$$K_{\text{eff}} + 2\pi M_S^2 = 0 \text{ at } T = T_R, \quad (4)$$

and can be deduced by means of diagrams as shown in Fig. 5. The resulting values are close to those displayed in Fig. 8. This means that the contribution from the directional entropy to the free energy^{11,12} must be very small in the present case. The phenomenological quantity K_S does not allow, *a priori*, an insight into its physical origin. It is not clear, why the perpendicular anisotropy appears for the (111) texture for the Fe layers, but not for the (110) texture. There is evidence, that misfit strain at the interfaces, via magnetostriction, contributes to the surface anisotropy K_S ,³⁹ similarly as it was predicted by Chappert and Bruno⁵ for incoherent interfaces, as they appear in the present layer system. The variation of the reorientation temperature T_R with the thickness of the individual Fe and CeH₂ layers can be understood only qualitatively at present: supplementing Eq. (3) by the term describing the magnetostatic interaction between the Fe layers, $2\pi M_S^2 = 2\pi M_{S,\text{Fe}}^2 t_{\text{Fe}}^2 / \Lambda^2$, replacing the volume anisotropy term K_V by the shape anisotropy of the Fe layers, $(-2\pi M_{S,\text{Fe}}^2)$, and referring the energy densities uniquely to the Fe layer volume, we have

$$\begin{aligned} (K_{\text{eff}} + 2\pi M_S^2) \frac{\Lambda}{t_{\text{Fe}}} &= \frac{2K_S}{t_{\text{Fe}}} + 2\pi M_{S,\text{Fe}}^2 \left[\frac{t_{\text{Fe}}}{t_{\text{Fe}} + t_{\text{CeH}_2}} - 1 \right] \\ &= K_{\text{eff}}^*. \end{aligned} \quad (5)$$

This equation compares the different competing contributions to the magnetic anisotropy density of the multilayers. In the perpendicular magnetic domain state, K_{eff}^* , which denotes the sum of the (positive) interface-anisotropy term $2K_S/t_{\text{Fe}}$ and the second (negative) volume term, is always positive. With increasing thickness of the *magnetic* layers t_{Fe} , K_{eff}^* is reduced. As a result, the stability of the perpendicular magnetic state is diminished and the reorientation temperature T_R decreases (see Fig. 5). The magnetostatic interaction term in Eq. (5), $2\pi M_{S,\text{Fe}}^2 t_{\text{Fe}} / (t_{\text{Fe}} + t_{\text{CeH}_2})$, and as a consequence the stability of the perpendicular state and hence T_R , is similarly reduced with increasing thickness of the *non-magnetic* layers t_{CeH_2} , and Eq. (5) approaches Eq. (3). This means that for large thicknesses of the CeH₂ sublayers, the perpendicular anisotropy originates entirely from the interface anisotropy, and the reorientation temperature $T_R(t_{\text{CeH}_2})$ should merge into a constant value which is independent of t_{CeH_2} . The data in Fig. 8(b) for multilayers with 16 Å thick Fe layers follow the form $T_R \propto t_{\text{CeH}_2}^{-1}$, which vanishes in the limit $t_{\text{CeH}_2} \rightarrow \infty$. This is consistent with the plots of Eq. (3) in Fig. 4, which shows

that 16 Å thick Fe sublayers are just at the upper limit where a perpendicular magnetic easy axis ($K_{\text{eff}} > 0$) in the multilayers can be stabilized by the interface anisotropy alone. The perpendicular magnetic state observed for this and larger Fe-layer thicknesses then results because the magnetostatic interaction between the domains across the CeH₂ spacer layers adds to the interface anisotropy. Let us finally mention that there is at present no explanation for the linear variation of T_R with t_{Fe}^{-1} or $t_{\text{CeH}_2}^{-1}$, respectively (Fig. 8).

IV. CONCLUSIONS

The present investigation shows that in the low-temperature magnetic ground state in structures of periodically stacked CeH₂ and Fe layers with pronounced (111) texture the magnetization is oriented perpendicular to the layer planes in a multidomain configuration. This is one of the rare cases where the phenomenon of perpendicular magnetic anisotropy has been observed for Fe layers with a preferred (111) orientation. We demonstrate in a phenomenological interpretation, that the perpendicular magnetic easy axis is a consequence not only of a strong interface contribution to the anisotropy, but also of an effect from the magnetostatic interaction between the domains in the Fe layers across the CeH₂ spacer layers. At a critical temperature T_R , which decreases with both the Fe or CeH₂ layer thicknesses, the magnetization

changes from the out-of-plane to an in-plane orientation. The experimentally observed linear variation of T_R with the reciprocal values of these thicknesses must remain unexplained at present. The present multilayer system is a particular case, where we have clearly demonstrated that a significant anisotropy contribution from a magnetostatic interaction between perpendicular domains in the Fe layers across the nonmagnetic spacer layers adds to the interface anisotropy to stabilize a perpendicular magnetic ground state. As a result, this state is observed to remarkably high thicknesses of the Fe layers. Furthermore, the system is outstanding among the rare-earth/iron multilayers, because the reorientation transition of the magnetization occurs rather abruptly in a narrow temperature interval, while in other cases the magnetization vector turns gradually in a broad temperature range and frequently does not always reach a truly perpendicular orientation (see, e.g., Ref. 24).

ACKNOWLEDGMENTS

This work was supported by the Deutsche Forschungsgemeinschaft within SFB 345. We thank R. Hassdorf for useful discussions. A very helpful and instructive conversation in the early stage of the experiments with Professor U. Gradmann is gratefully acknowledged.

*Now at Hahn-Meitner-Institut, Glienicke Str. 100, 14109 Berlin, Germany.

¹See, e.g., *Ultrathin Magnetic Structures*, edited by J. A. C. Bland and B. Heinrich (Springer, Berlin, 1994), Vol. I, Chap. 2.

²L. Néel, *J. Phys. Radium* **15**, 225 (1954).

³See, J. G. Gay, R. Richter, G. H. O. Daalderop, P. J. Kelly, and M. F. H. Schuurmans, in *Ultrathin Magnetic Structures*, edited by J. A. C. Bland and B. Heinrich (Springer, Berlin, 1994), Vol. I, pp. 21–65.

⁴G. H. O. Daalderop, P. J. Kelly, and F. J. A. den Broeder, *Phys. Rev. Lett.* **68**, 682 (1992).

⁵C. Chappert and P. Bruno, *J. Appl. Phys.* **64**, 5736 (1988).

⁶R. Jungblut, M. T. Johnson, J. aan de Stegge, A. Reinders, and F. J. A. den Broeder, *J. Appl. Phys.* **75**, 6424 (1994).

⁷D. P. Pappas, K.-P. Kämper, and H. Hopster, *Phys. Rev. Lett.* **64**, 3179 (1990).

⁸R. Allenspach and A. Bischof, *Phys. Rev. Lett.* **69**, 3385 (1992).

⁹Z. Q. Qiu, J. Pearson, and S. D. Bader, *Phys. Rev. Lett.* **70**, 1006 (1993).

¹⁰See, e.g., A. Moschel and K. D. Usadel, *Phys. Rev. B* **49**, 12 868 (1994), and references therein.

¹¹P. J. Jensen and K. H. Bennemann, *Phys. Rev. B* **42**, 849 (1990).

¹²P. J. Jensen and K. H. Bennemann, *Solid State Commun.* **83**, 1057 (1992).

¹³C. Kittel, *Phys. Rev.* **70**, 965 (1946).

¹⁴R. Allenspach, *J. Magn. Magn. Mater.* **129**, 160 (1994), and references therein.

¹⁵J. R. Barnes, S. J. O'Shea, M. E. Welland, J.-Y. Kim, J. E.

Evetts, and R. E. Somekh, *J. Appl. Phys.* **76**, 2974 (1994).

¹⁶Y. Yafet and E. M. Gyorgy, *Phys. Rev. B* **38**, 9145 (1988).

¹⁷A. Kashuba and V. L. Pokrovsky, *Phys. Rev. Lett.* **70**, 3154 (1993); *Phys. Rev. B* **48**, 10 335 (1993).

¹⁸B. Kaplan and G. A. Gehring, *J. Magn. Magn. Mater.* **128**, 111 (1993).

¹⁹H. J. G. Draaisma and W. J. M. de Jonge, *J. Appl. Phys.* **62**, 3318 (1987).

²⁰K. Cherifi, C. Dufour, M. Piecuch, A. Bruson, Ph. Bauer, G. Marchal, and Ph. Mangin, *J. Magn. Magn. Mater.* **93**, 609 (1991).

²¹Y. J. Wang and W. Kleeman, *Phys. Rev. B* **44**, 5132 (1991).

²²L. T. Baczewski, M. Piecuch, J. Durand, G. Marchal, and P. Delcroix, *Phys. Rev. B* **40**, 11 237 (1989).

²³K. Mibu, N. Hosoito, and T. Shinjo, *Hyperfine Interact.* **54**, 831 (1990).

²⁴Y. J. Wang, C. P. Luo, W. Kleemann, B. Scholz, R. A. Brand, and W. Keune, *J. Appl. Phys.* **73**, 6907 (1993).

²⁵J. Thiele, F. Klose, A. Schurian, O. Schulte, W. Felsch, and O. Bremert, *J. Magn. Magn. Mater.* **119**, 141 (1993).

²⁶F. Klose, J. Thiele, A. Schurian, O. Schulte, M. Steins, O. Bremert, and W. Felsch, *Z. Phys. B* **90**, 79 (1993).

²⁷Ph. Bauer, F. Klose, O. Schulte, and W. Felsch, *J. Magn. Magn. Mater.* **138**, 163 (1994).

²⁸F. Klose, M. Steins, T. Kacsich, and W. Felsch, *J. Appl. Phys.* **74**, 1040 (1993).

²⁹R. Hassdorf, M. Arend, and W. Felsch, *Phys. Rev. B* **51**, 8715 (1995).

³⁰A. Weidinger and D. Nagengast (unpublished).

³¹J. Landes, Ch. Sauer, B. Kabius, and W. Zinn, *Phys. Rev. B* **44**, 8342 (1991).

- ³²S. Handschuh, J. Landes, U. Köbler, Ch. Sauer, G. Kisters, A. Fuss, and W. Zinn, *J. Magn. Magn. Mater.* **119**, 254 (1993).
- ³³F. Klose, O. Schulte, F. Rose, W. Felsch, S. Pizzini, C. Giorgetti, F. Baudelet, E. Dartyge, G. Krill, and A. Fontaine, *Phys. Rev. B* **50**, 6174 (1994).
- ³⁴F. Baudelet, F. Manar, O. Schulte, C. Giorgetti, E. Dartyge, G. Krill, and W. Felsch (unpublished).
- ³⁵W. Lohstroh, O. Schulte, B. Damaske, W. Felsch, F. Klose, and H. Maletta, *Physica B* (to be published).
- ³⁶A. Suna, *J. Appl. Phys.* **59**, 313 (1986).
- ³⁷C. Kooy and U.ENZ, *Philips Res. Rep.* **15**, 7 (1960).
- ³⁸H. J. G. Draaisma, W. J. M. de Jonge, and F. J. A. den Broeder, *J. Magn. Magn. Mater.* **66**, 351 (1987).
- ³⁹R. Hassdorf, M. Arend, U. Geyer, U. von Hülsen, O. Schulte, and W. Felsch (unpublished).